ACS Sustainable Chemistry & Engineering

Research Article

Cite This: ACS Sustainable Chem. Eng. 2019, 7, 5002−5009

pubs.acs.org/journal/ascecg

Dehydroabietylamine-Based Cellulose Nanofibril Films: A New Class of Sustainable Biomaterials for Highly Efficient, Broad-Spectrum Antimicrobial Effects

Ghada Hassan,[†] Nina Forsman,[‡] Xing Wan,[§] Leena Keurulainen,[†] Luis M. Bimbo,[#] Leena-Sisko Johansson,[‡] Nina Sipari,[∥] Jari Yli-Kauhaluoma,[†] Ralf Zimmermann,[⊥] Susanne Stehl,[⊥] Carsten Werner,[⊥] Per E. J. Saris,[§] Monika Österberg,*[,‡] and Vânia M. Moreira*[,†,#]

[†]Drug Research Program, Division of Pharmaceutical Chemistry and Technology, Faculty of Pharmacy, University of Helsinki, Viikinkaari 5 E, P.O. Box 56, FI-00014 Helsinki, Finland

[‡]Department of Bioproducts and Biosystems, Aalto University, Vuorimiehentie 1, P.O. Box 16300, FI-00076 Aalto, Finland

[§]Department of Microbiology, Faculty of Agriculture and Forestry, University of Helsinki, Viikinkaari 9, P.O. Box 56, FI-00014 Helsinki, Finland

[∥]Viikki Metabolomics Unit, Faculty of Biological & Environmental Sciences, University of Helsinki, Viikinkaari 5 E, P.O. Box 56, FI-00014 Helsinki, Finland

[⊥]Leibniz Institute of Polymer Research Dresden, Max Bergmann Center for Biomaterials Dresden, Hohe Strasse 6, 01069 Dresden, Germany

[#]Strathclyde Institute of Pharmacy and Biomedical Sciences, University of Strathclyde, 161 Cathedral Street, G4 0RE Glasgow, United Kingdom

Supporting Information

ABSTRACT: The design of antimicrobial surfaces as integral parts of advanced biomaterials is nowadays a high research priority, as the accumulation of microorganisms on surfaces inflicts substantial costs on the health and industry sectors. At present, there is a growing interest in designing functional materials from polymers abundant in nature, such as cellulose, that combine sustainability with outstanding mechanical properties and economic production. There is also the need to find suitable replacements for antimicrobial silver-based agents due to environmental toxicity and spread of resistance to metal antimicrobials. Herein we report the unprecedented decoration of cellulose nanofibril (CNF) films with dehydroabietylamine **1** (**CNF-CMC-1**), to give an innovative contact-active surface active against Gram-positive and Gram-negative bacteria including the methicillin-resistant *S. aureus* MRSA14TK301, with low potential to spread resistance and good biocompatibility, all achieved with low surface coverage. **CNF-CMC-1** was particularly effective against *S. aureus* ATCC12528, causing virtually complete reduction of the total cells from 10^5 colony forming units (CFU)/mL bacterial suspensions, after 24 h of contact. This gentle chemical modification of the surface of CNF fully retained the beneficial properties of the original film, including moisture buffering and strength, relevant in many potential applications. Our originally designed surface represents a new class of ecofriendly biomaterials that optimizes the performance of CNF by adding antimicrobial properties without the need for environmentally toxic silver.

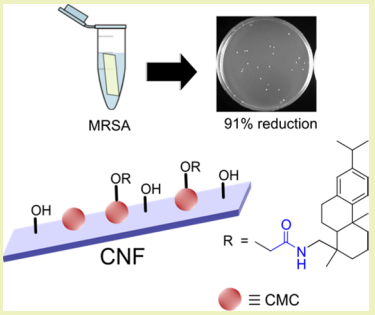

KEYWORDS: *Nanocellulose, Dehydroabietylamine, Antimicrobial, Drug-resistant, Silver, Biomaterials*

INTRODUCTION

Preventing the accumulation of microorganisms on surfaces is critical in many different applications including textiles, furniture, food packaging, and industrial and marine equipment.[1,2] Therefore, there is a pressing need for antimicrobial surfaces that can efficiently prevent and/or eliminate fouling by bacteria, to reduce health risks, extend the life span of consumer/industrial goods, and allow for general convenience. In the design of new antibacterial surfaces or as a means to enhance the performance of existing ones, a plethora of strategies have been reported that include surface coating, chemical modification, or patterning.[3−9] Common drawbacks include failure in achieving efficacy and biocompatibility levels suitable for specific target applications, extreme chemical complexity that reflects on cost-effectiveness, and, last but not the least, the use of synthetic polymers and/or environmentally hazardous reaction conditions.

Received: November 1, 2018
Revised: February 1, 2019
Published: February 4, 2019

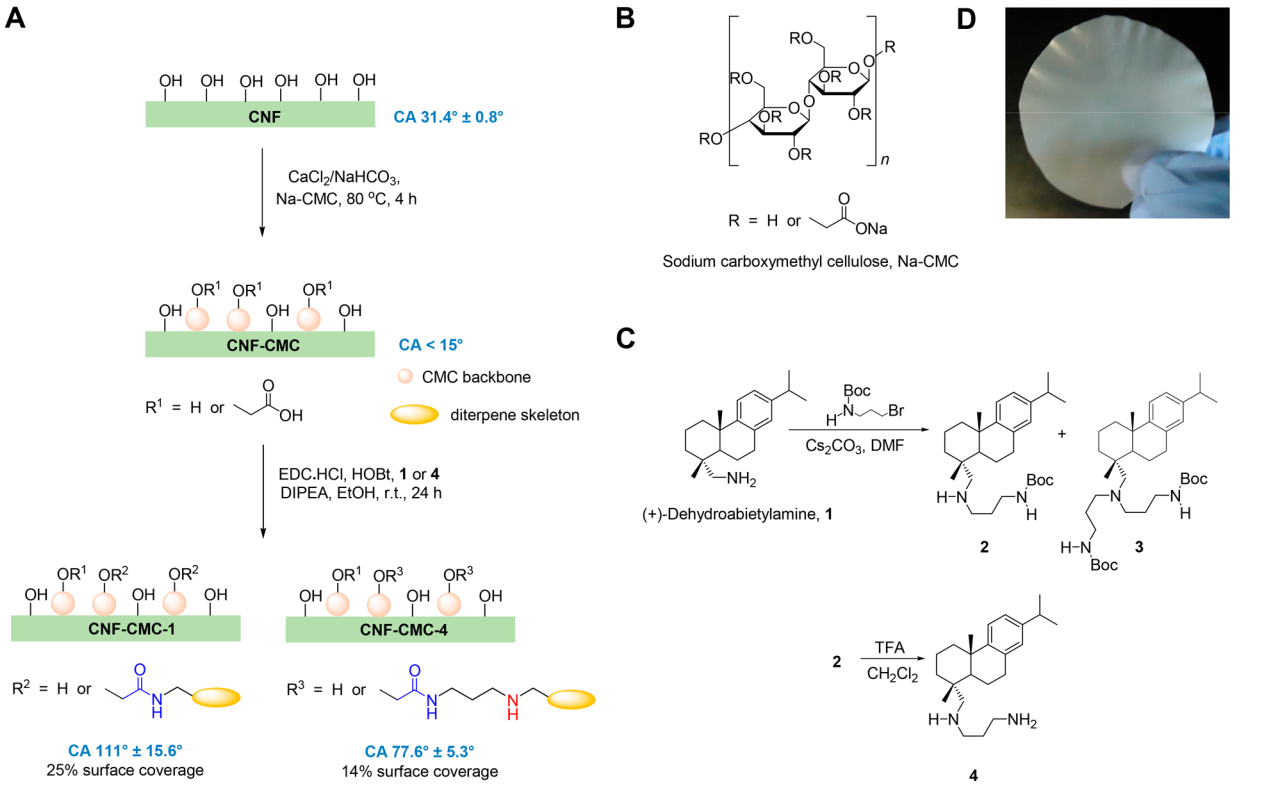

Figure 1. A. Synthesis of **CNF-CMC-1** and **CNF-CMC-4**. Contact angle values measured at 5 s and expressed as mean ± standard deviation. Degree of surface coverage based on C−C content in XPS analysis. **B**. Sodium carboxymethylcellulose (Na-CMC). **C** Synthesis of compound **4** from (+)-dehydroabietylamine **1**. **D**. Example picture of the hybrid nanocellulose surfaces (**CNF-CMC-4**).

Cellulose, with an estimated production of 1.5×10^{12} tons in the biosphere annually, is the most abundant naturally occurring polymer on earth and a virtually inexhaustible source of raw material for the design of environmentally friendly and biocompatible products to replace fossil fuel derived ones.[10] Cellulose nanofibril (CNF) is considered as an advanced, fully renewable material with high potential to reach commercial applications in a nearby future.[11−17] CNF is prepared by mechanical disintegration of cellulose fibers via high shearing followed by homogenization and can nowadays be obtained from either wood or crops with reasonably low energy consumption. The appealing properties of CNF, including global abundance and renewability as well as high stiffness and lightweight character, are a consequence of both its natural origin and its chemical structure, i.e. of the way it is organized into fibrils with length in the micrometer and width in the nanometer range, forming a network with both amorphous and crystalline regions. In particular, thin films can be made of CNF that are robust, solvent-resistant, and can be surface-modified for acquiring functionality.[18] Target markets for CNF films, as a sustainable alternative to synthetics, are diverse and include flexible electronics, the automotive and aerospace industries (for instance in light-weight plane fabrication), and medical devices as well as food packaging.[11−16] In all these applications, it is desirable that the films are gifted with antimicrobial activity as CNF itself does not possess this property thus hampering its potential use.

Although several chemical modifications have been described for decoration of the surface of CNF with small molecules, proteins, or polymers,[11−16] some leading to antibacterial properties,[13] the direct functionalization of CNF films for the production of materials with antimicrobial properties remains largely unexplored to date. The few available reports describe the preparation of antimicrobial CNF mainly by physical adsorption of metal nanoparticles,[19,20] especially those comprising silver,[13,21−23] that act by killing bacteria once released from the material during the course of time. A few others rely on grafting proteins[16,24] or highly cationic compounds[25] onto its surface. Despite the fact that it is effective, silver is highly toxic to aquatic organisms and there are major concerns about the spread of antimicrobial resistance due to its continued use as well as toxicity toward humans following long-term exposure.[26,27] Moreover, polycations are typically poorly biocompatible, whereas enzymes suffer from chemical instability. Herein we report the design and synthesis of innovative antimicrobial CNF films based on modification of their surface with (+)-dehydroabietylamine **1** (Figure 1), a commercially available diterpenic amine used as a chiral resolving agent for carboxylic acids, which we have previously shown to possess antimicrobial properties.[28,29] Our work shows that contact-active, broad-spectrum antimicrobial activity, and good biocompatibility can be achieved without the need for extensive film surface coverage with the diterpene, and we discuss plausible mechanisms of action and applications in the biomedical field. To the best of our knowledge this is the first report on the modification of CNF with dehydroabietylamine **1** and related compounds.

RESULTS AND DISCUSSION

Carbodiimide chemistry was selected in order to couple **1** to CNF after irreversible adsorption[30] of sodium carboxymethyl cellulose (Na-CMC) to the film surface (Figure 1A−C). The

DOI: 10.1021/acssuschemeng.8b05658
ACS Sustainable Chem. Eng. 2019, 7, 5002−5009

reaction with Na-CMC, carried out in low salt concentration aqueous solution, enriched the surface of the films in carboxyl groups that were then covalently linked to **1** through the amidation reaction. Both methods employ relatively nontoxic and inexpensive reagents and ethanol, an environmentally preferable solvent,[31] was used in the second step instead of *N*,*N*-dimethylformamide (DMF), the usual solvent of choice for coupling reactions.

Contact angle (CA) measurements at 5 s provided a rough estimate of the success of the modification, as it was expected that the binding of **1** to the surface of the CNF film would render it more hydrophobic due to an increase in carbon content (Figure 2A). Indeed, the CA value was much higher

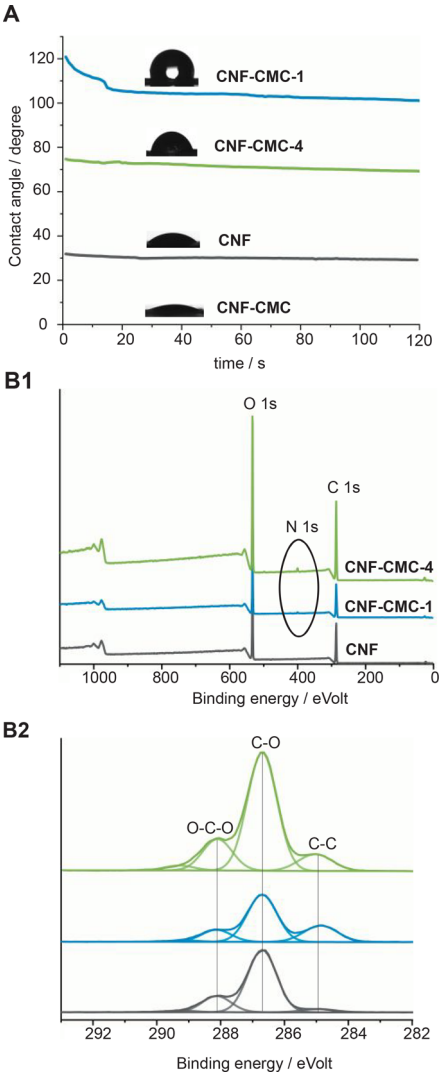

Figure 2. Contact angle (A) and XPS wide scan (B1) and high resolution C 1s (B2) as a graph for representative samples.

for **CNF-CMC-1** than for **CNF** and **CNF-CMC**. X-ray photoelectron spectroscopy (XPS) analysis revealed that the modified CNF surface in **CNF-CMC-1** contained nitrogen and carbon atoms bound only to other carbon atoms with no bonds to oxygen (C−C), inexistent in cellulose (and therefore in CNF), which could only have originated from our chemical modification (Figure 2B1−B2, Table 1). **CNF-CMC-1** also displayed lower content of carbon atoms with one bond to oxygen than the reference film. We estimated that compound **1**

Table 1. High Resolution Numerical XPS Data

	Wide Scan Atomic Concentrations (%)			
sample	C 1s	O 1s	N 1s	Si 2p
CNF	60.7	39.3	0.0	0.0
CNF-CMC-1	67.0	32.1	0.9	0.0
CNF-CMC-4	62.2	35.9	1.3	0.7
	High Resolution C 1s Carbon Fits			
sample	C—C	C—O	O—C—O	O—C═O
CNF	4.4	74.5	19.2	1.9
CNF-CMC-1	25.0	58.4	14.9	1.7
CNF-CMC-4	13.9	66.5	17.2	2.5

covered only 20% of the surface based on the N content and 25% based on C−C content, indicating very low surface coverage.

In line with the low coverage value, atomic force microscopy (AFM) height images (Figure 3A) showed that the surface of cellulose fibrils on **CNF-CMC-1** did not significantly differ from that of CNF. Fourier-transform infrared spectroscopy (FTIR) analysis furthermore verified that only the outermost surface was modified, since no dramatic changes were detected between modified and unmodified films (Figure 3B). The ability to permeate gas or vapor and the mechanical properties of **CNF-CMC-1** were also not significantly affected when compared to CNF (Table S1) apart from a slightly higher oxygen permeability (OP) value at low (50%) relative humidity (RH), which is consistent with the increase in the hydrophobicity of the films after modification with **1** that results in the ability to attract a higher number of oxygen molecules. It is generally accepted that high surface roughness and low surface energy increase hydrophobicity.[32] In **CNF-CMC-1**, the hydrophobicity is most likely caused by the particular surface chemistry, as the AFM data showed no significant changes in surface roughness. The lack of impact of the modification of CNF with **1** on the barrier performance is yet another reflection of the low surface coverage as an increase in this performance in humid environment can only be attained if the CNF film surface is fully covered.[33]

Overall, the surface modification of CNF with **1** was gentle, yet effective, producing an increase in hydrophobicity that did not result in deterioration of the breathability, i.e., the film's water vapor and oxygen gas permeability,[34] nor of the moisture buffering properties, i.e., the film's ability to adsorb and release moisture in the surrounding environment thus dampening changes in relative humidity,[35] which are beneficial for many applications.[33] This is in sharp contrast with modifications made with hydrophobic compounds prior to film formation that typically disturb the hydrogen bonding network resulting in loss of both barrier and strength performance.[36]

CNF-CMC-1 showed clear and robust antimicrobial activity against different bacterial strains including the Gram positive *Staphylococcus aureus*, the Gram negative *Escherichia coli*, and the methicillin-resistant *S. aureus* MRSA14TK301, whereas CNF and **CNF-CMC** were inactive (Figure 4A). **CNF-CMC-1** was particularly effective against *S. aureus* ATCC12528 where reduction of the total cells from 10^5 CFU/mL bacterial suspensions was virtually complete after 24 h of contact. Potent activity was also observed against the methicillin-resistant strain and *E. coli*, however less pronounced than that observed against the normal *S. aureus* strains. **CNF-CMC-1** did not endure treatment with strong acid but retained antimicrobial activity even after exposure to different solvents,

DOI: 10.1021/acssuschemeng.8b05658
ACS Sustainable Chem. Eng. 2019, 7, 5002−5009

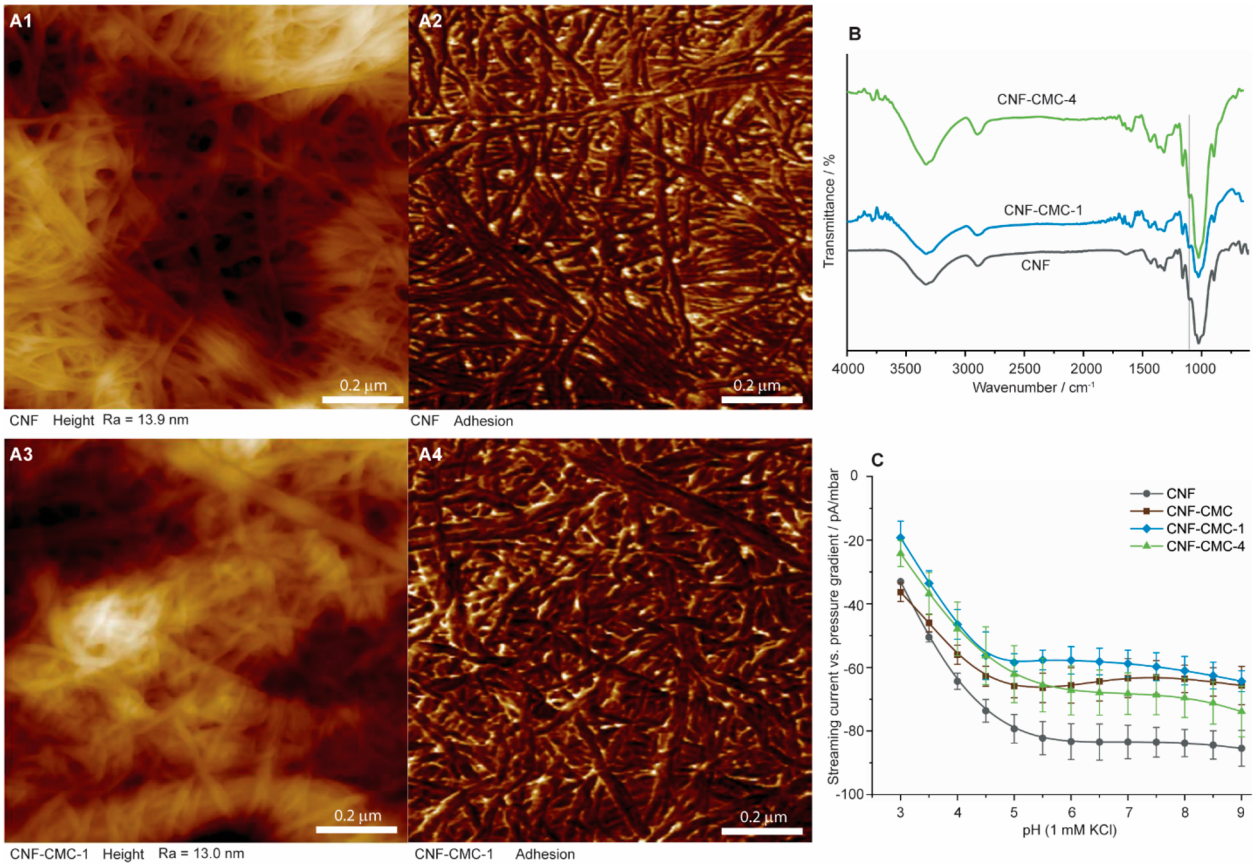

Figure 3. AFM images (A1, A3 height; A2, A4 adhesion), FTIR spectra (B), and streaming current *vs* pressure gradient (C) for representative samples.

including strong base, at room temperature, for 24 h (Table S2).

In contrast, compound **1** is a relatively weak antimicrobial agent against the tested strains, with minimal inhibitory concentrations (MIC) values in the 40−50 μM range (Table S3, Figure 5A). Incubation of either *S. aureus* ATCC12598 or *E. coli* DH5α with 100 μM of **1**, for 4 h, resulted in death of some bacteria in the medium, with slight leakage of ATP from *S. aureus* cells, suggesting that **1** is a slow acting compound (Figure 5B).

The factors governing bacterial interaction with surfaces are well-known and include surface charge, hydrophobicity, topography, and chemical environment.[2,37] Streaming current measurements (Figure 3C) revealed the typical electrokinetic fingerprint of an oxidized cellulose[38] for **CNF**, **CNF-CMC**, and **CNF-CMC-1**. The point of zero streaming current was found below pH 3, and the current reached a plateau in the neutral and alkaline pH range indicating that all surfaces are negatively charged under the conditions of the bacterial assay. Compared to **CNF**, a slightly lower negative streaming current was measured for **CNF-CMC** and **CNF-CMC-1** as a result of the increased friction exerted by the soft CMC layer[39] on the hydrodynamic flow at the interface.[40] In view of the electrokinetics and AFM data, surface charge and topography do not seem to be determinants of the antimicrobial activity of **CNF-CMC-1**.

To probe the impact of small changes in chemical environment at the CNF films surface, we synthesized **CNF-CMC-4** using compound **4** (Figure 1C−D), a derivative of **1**, in order to determine the effects of exposing a protonable amino group at the surface of the CNF, as the presence of cationic groups in antimicrobials is known to result in increased potency albeit accompanied by potential toxicity.[2] Compound **4** was made from **1** as depicted on Figure 1C. As before, the XPS analysis confirmed the desired modification and coverage was calculated as 18% based on N and 14% based on C−C (Figure 2B1−B2, Table 1). In this case, the steric orientation of compound **4** at the surface of CNF is unknown and probably differs between molecules, as there is mobility in the carbon chain between the two N atoms, which further hampers calculation. In **CNF-CMC-4**, the increase in the CA value was less pronounced than in **CNF-CMC-1** (Figure 2A) and the electrokinetic fingerprint was similar to that of **CNF-CMC** and **CNF-CMC-1** (Figure 3C), building up the evidence for low decoration of the surface with **1** or **4**. Nonetheless, the inclusion of **4** at the surface of CNF films dramatically impacted Gram positive staphylococci cells, which were killed after 24 h of contact with **CNF-CMC-4** (Figure 4A). A sharp reduction (98.3% of total cells) from the suspension of methicillin-resistant *S. aureus* MRSA 14TK301 and *E. coli* (99.9%) was also observed. We found that the antimicrobial potency of **4** was only moderately better than that of compound **1**, with MIC values still in the high micromolar range (Table S3, Figure 5A). However, bacterial cell death with ATP efflux in *S. aureus* ATCC12598 was much more evident after treatment with **4**, indicating that this compound causes bacterial membrane disruption rapidly (Figure 5B).

As depicted on Figure 4B, the cell surface became rough after treatment with compound **1** for 1 h when compared to untreated *S. aureus*, whereas treatment with **4** caused

DOI: 10.1021/acssuschemeng.8b05658
ACS Sustainable Chem. Eng. 2019, 7, 5002−5009

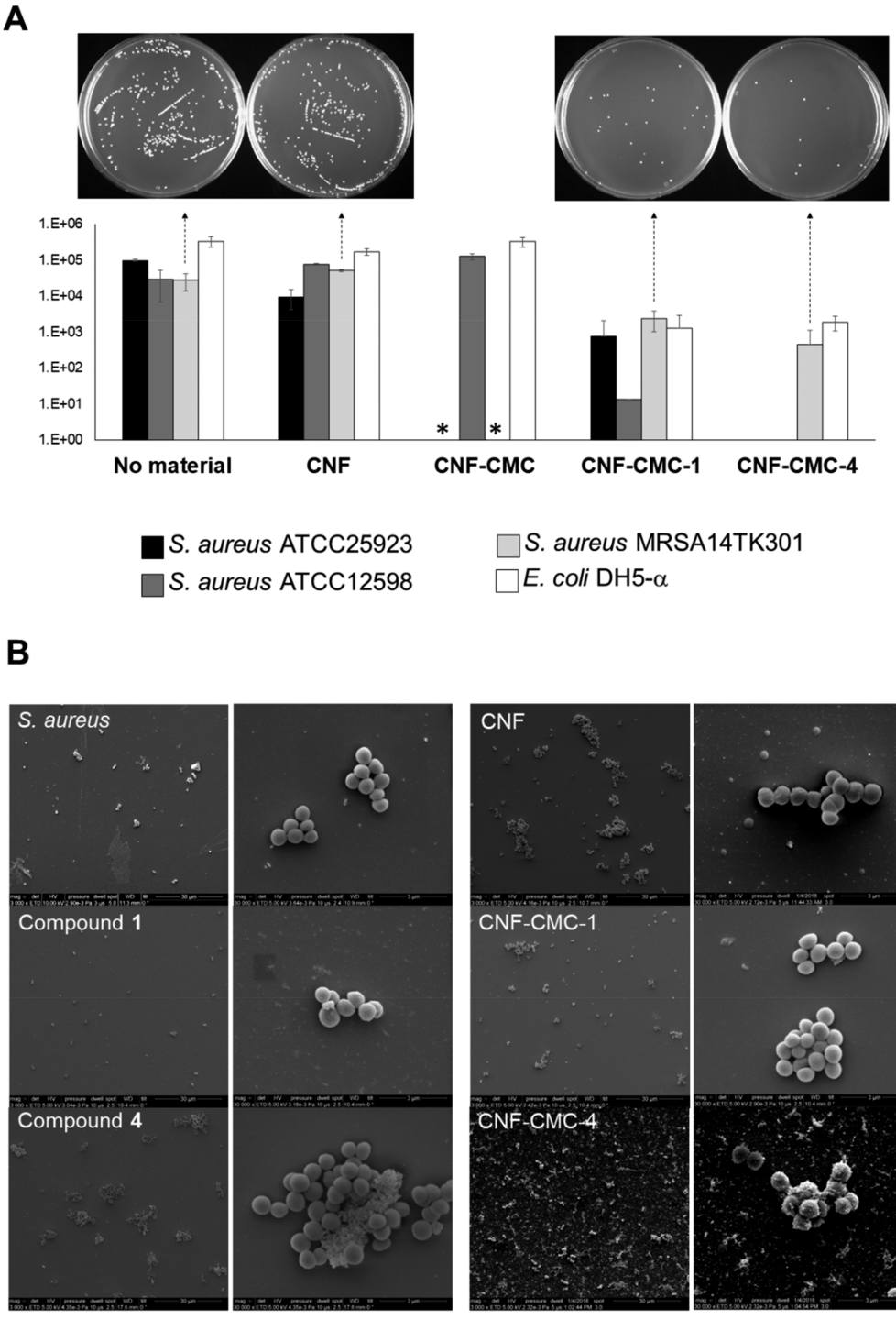

Figure 4. A. Antimicrobial activity of **CNF**, **CNF-CMC**, **CNF-CMC-1**, and **CNF-CMC-4**. After 24 h incubation, the amount of viable *S. aureus* MRSA 14TK301 from 10% of ~10^5 CFU/mL cell suspensions is shown in the plate pictures above. * not tested. **B.** *S. aureus* ATCC12598 (~10^8 CFU/mL) under scanning electron microscope after treatment with **1** or **4** (100 μM, 1 h) and **CNF**, **CMF-CMC-1**, or **CNF-CMC-4** (24 h). Left of each panel, 3000× magnification; right of each panel, 30 000× magnification.

significant morphological changes on the cells and obvious debris appeared. The bacterial cells contacted with CNF looked unharmed especially when compared to those incubated with **CNF-CMC-4**, were abundant debris was visible in the background and the few remaining cells look highly deformed. No significant changes where visible on the cells in contact with **CNF-CMC-1**. Moreover, biocompatibility assessment of **CNF-CMC-1** and **CNF-CMC-4** (Table 2) revealed that **CNF-CMC-1** was generally better tolerated by human erythrocytes than **CNF-CMC-4**, as the percent hemolysis caused was negligible. Human skin fibroblasts colonized **CNF-CMC-1** to an extent comparable to that observed with CNF, which is regarded as a biocompatible biomaterial.[11,14] For **CNF-CMC-4**, the hemolysis rate was 6.5% and in sharp contrast with **CNF-CMC-1**, fibroblasts did not proliferate on top of its surface.

Overall, the combination of **1** and **4** with CNF films resulted in hybrid surfaces displaying broad and potent antimicrobial

DOI: 10.1021/acssuschemeng.8b05658
ACS Sustainable Chem. Eng. 2019, 7, 5002−5009

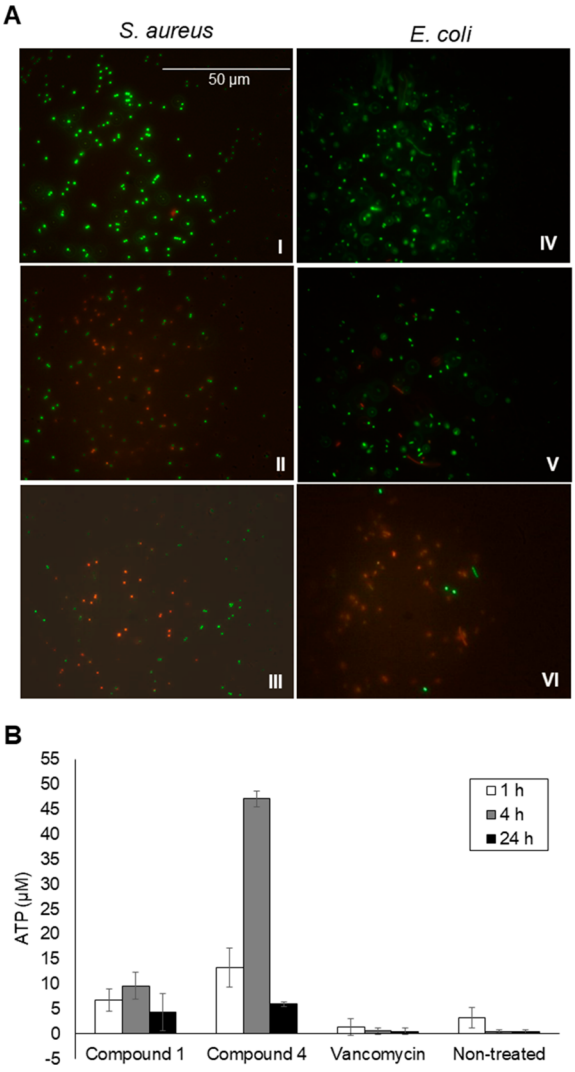

Figure 5. A. Fluorescence microscopy image of bacteria counts with/without treatment with compounds **1** and **4**. **I** nontreated *S. aureus* ATCC12598; **II** *S. aureus* ATCC12598 incubated with compound **1** (100 μM) for 1 h; **III** *S. aureus* ATCC12598 incubated with compound **4** (100 μM) for 1 h; **IV** nontreated *E. coli* DH5α; **V** *E. coli* DH5α incubated with compound **1** (100 μM) for 1 h; **VI** *E. coli* DH5α incubated with compound **4** (100 μM) for 1 h. **B**. Efflux of ATP from *S. aureus* ATCC12598 after incubation with compounds **1** and **4** (100 μM). Bacteriostatic vancomycin with 100 μM final concentration was used as control.

activity despite the low coverage. The differences observed in the activity and biocompatibility of **CNF-CMC-1** and **CNF-CMC-4** clearly show that small changes in the diterpene used for the functionalization, more than charge, topography or hydrophobicity, will significantly impact the chemical environment at the surface, thus modulating the interaction of the films with bacterial and eukaryotic membranes. A physicochemical mode of action such as membrane disruption or interaction with surface molecules seems plausible, in light of the broad spectrum of activity with low surface coverage, and the unlikelihood that the physically bound compounds at the surface could breach into the bacterial cells. XPS analysis of **CNF-CMC-1** and **CNF-CMC-4** recovered after contact with the bacteria by washing with water and ethanol followed by drying, suggest that the surface of **CNF-CMC-1** was mostly unharmed whereas some change in surface structure for **CNF-CMC-4** occurred (Table S4), which could result from wearing off after contact with the bacteria or from bacterial debris indwelling at the surface, causing changes to the chemical composition.

CONCLUSION

Herein we set the grounds for a facile, ecofriendly, and mild strategy for immobilization of antimicrobial diterpenes onto CNF, leading to innovative and sustainable silver-free antibacterial films, without compromising the original physicochemical properties of the nanocellulose. The proposed mode of action, along with the fact that the films are based on compounds from a new chemical class, should account for a low potential to spread resistance. Furthermore, the potency and biocompatibility of **CNF-CMC-1** warrant additional investigation for applications in the biomedical field where surfaces able to minimize the risk of infection at relevant bacterial bioburden are needed. Efforts are currently underway to investigate this possibility as well as the applicability of our design strategy to other biopolymers.

EXPERIMENTAL SECTION

Chemistry. *General.* (+)-Dehydroabietylamine was purchased from TCI, Europe. *N,N*-Diisopropylethylamine (DIPEA), 1-hydroxybenzotriazole hydrate (HOBt), di-*t*-butyl dicarbonate, cesium carbonate, sodium carboxymethyl cellulose (DS 0.70−0.85, MW ∼ 250 000), *N,N*-dimethylformamide (DMF), and dichloromethane were acquired from Sigma-Aldrich Co. 3-Bromopropylamine hydrobromide was purchased from Ega-Chemie. *N*-(3-Dimethylaminopropyl)-*N*′-ethylcarbodiimide hydrochloride (EDC) and trifluoroacetic acid (TFA) were purchased from Fluorochem Ltd. Calcium chloride was purchased from Merck, sodium hydrogen carbonate, from VWR International Oy, methanol, from VWR Chemicals, and ethanol (Etax A, 94% w/w), from Altia Oyj. All reagents were used without purification apart from dehydroabietylamine, which was purified by flash column chromatography (FCC) using an ethyl acetate: 10% w/w NH_4OH in methanol gradient 10 → 60%, when used as the starting material for the synthesis of compound **4.** For thin layer chromatography (TLC) silica gel 60 F254 was used. FCC was made with a Biotage high-performance flash chromatography Sp4-system (Uppsala, Sweden) using a 0.1 mm path length flow cell UV detector/recorder module (fixed wavelength: 254 nm), and 25, 50, or 100 g SNAP cartridges (25−100 mL/min flow rate).

Table 2. Biocompatibility Assessment

assay	CNF	CNF-CMC-1	CNF-CMC-4	Triton X-100 2%
Hemolysis[a,c]	0	0.9 ± 0.6	6.5 ± 1.9**	100 ± 3.0***
Fibroblast proliferation 72 h[b,c]	59.8 ± 7.3	47.2 ± 17.7	2.7 ± 0.4***	1.2 ± 0.4***

[a]Measured in terms of percent of hemolyzed erythrocytes. [b]Measured in terms of percent of viable fibroblasts placed on top of each material compared with the percent of viable fibroblasts grown on a sterile tissue culture-treated 24-well plate. [c]Statistical analysis was made by ANOVA, followed by a Dunnett's multiple comparison test. All data sets were compared with **CNF** for both hemolysis and fibroblast proliferation. The level of significance was set at probabilities of * $p < 0.05$, ** $p < 0.01$, and *** $p < 0.001$.

DOI: 10.1021/acssuschemeng.8b05658
ACS Sustainable Chem. Eng. 2019, 7, 5002−5009

Infrared (IR) spectra were recorded on a Vertex 70 (Bruker Optics Inc., MA, USA) FTIR instrument with a horizontal attenuated total reflectance (ATR) accessory (MIRacle, Pike Technology, Inc., WI, USA). The transmittance spectra were recorded at a 4 cm^{-1} resolution, between 4000 and 600 cm^{-1}, using the OPUS 5.5 software (Bruker Optics Inc., MA, USA). The graphs in Figure 3B are normalized by the 1159 cm^{-1} band. Nuclear magnetic resonance (NMR) spectra were recorded on a Bruker Ascend 400 spectrometer, in $CDCl_3$, with tetramethylsilane (TMS) as the internal standard. The chemical shifts are reported in parts per million (ppm) and on the δ scale from TMS as an internal standard. The coupling constants J are quoted in Hertz (Hz). Exact mass analyses were performed with a Waters Acquity UPLC attached to Synapt G2 HDMS in positive ionization (ESI) mode (Waters, MA, USA).

Preparation of CNF films. Never-dried birch kraft pulp was used to prepare a CNF dispersion. To control the counterion type and ionic strength, the pulp was washed into sodium form prior to disintegration but was not chemically or enzymatically pretreated.[41] The pulp was disintegrated using a high-pressure fluidizer (Microfluidics, M-110Y, Microfluidics Int. Co., Newton, MA) and circulated for 6 passes through the fluidizer. Free-standing CNF films were prepared by filtrating 100 mL of 0.85% CNF through a Sefar Nitex polyamine monofilament fabric with a 10-μm pore size, at 2.5 bar pressure, for 30 min. The film was then hot-pressed for 2 h at 100 °C and 1800 kg/cm^2 pressure in a Carver Laboratory press (Fred S. Carver Inc.). The prepared films were stored at standard conditions (23 °C and 50% RH). More detailed information about freestanding CNF films and their production can be found elsewhere.[18] CNF films were cut into circles with a 5 cm diameter for the experiments reported below.

*Activation of the CNF Film Surface by Carboxymethylation (**CNF-CMC**).*[30] To a round-bottomed reaction flask containing a 0.05 M/0.01 M solution of $CaCl_2/NaHCO_3$ in water (75 mL), Na-CMC (270 mg) was added. The mixture was stirred for 5 min, at 80 °C. One CNF film circle was then added to the mixture and the left to agitate with magnetic stirring at 80 °C, for 4 h. The reaction mixture was poured out from the flask, and the CNF circle was washed with the following solutions under magnetic stirring at room temperature: deionized water (150 mL, 10 min), a 0.1 M solution of CH_3COOH in water (75 mL, 10 min), deionized water (150 mL, 10 min), a 0.4% solution of $NaHCO_3$ in water (75 mL, 1 h), and deionized water (150 mL, 10 min). The CNF film circle was recovered from the aqueous solution, placed between 2 blotting sheets, and left in an oven to dry overnight at 103 °C.

*Amidation of Activated CNF Films (**CNF-CMC-1** and **CNF-CMC-4**).* One CNF film circle activated as described above was added to a round-bottomed flask containing EDC hydrochloride (0.02 M) and HOBt (0.02 M) in 94% w/w ethanol (60 mL) and left under magnetic stirring at room temperature for 1 h. (+)-Dehydroabietylamine **1** or compound **4** (0.02 M) and DIPEA (0.04 M) were added, and the mixture was left to agitate at room temperature for additional 24 h. The reaction mixture was then poured out from the reaction flask and the CNF film circle was first rinsed with 94% w/w ethanol (20 mL) and then washed under magnetic stirring with deionized water (4 × 150 mL, 10 min each washing). The modified CNF film circle was recovered from the aqueous solution, placed between 2 blotting papers, and left in an oven to dry overnight at 103 °C.

■ ASSOCIATED CONTENT

Supporting Information

The Supporting Information is available free of charge on the ACS Publications website at DOI: 10.1021/acssuschemeng.8b05658.

Compound synthesis; Other experiments including the following: CA, streaming current measurements, XPS, AFM, OTR, WVTR, mechanical properties, microbiology, SEM, and biocompatibility; Oxygen and water vapor permeability, tensile strength, and Young's modulus data for **CNF** and **CNF-CMC-1** (Table S1); Antimicrobial activity of compounds **1** and **4** (Table S2); XPS data for **CNF-CMC-1** and **CNF-CMC-4** before and after bacterial exposure (Table S3); NMR spectra (PDF)

■ AUTHOR INFORMATION

Corresponding Authors

*Email: vania.moreira@strath.ac.uk. Tel.: +44 (0)141 548 4694 (V.M.M.).

*Email: monika.osterberg@aalto.fi. Tel.: +358-50-5497218 (M.O.).

ORCID

Luis M. Bimbo: 0000-0002-8876-8297

Jari Yli-Kauhaluoma: 0000-0003-0370-7653

Ralf Zimmermann: 0000-0003-4256-0754

Monika Österberg: 0000-0002-3558-9172

Vânia M. Moreira: 0000-0001-6169-5035

Notes

The authors declare no competing financial interest.

■ ACKNOWLEDGMENTS

V.M.M. acknowledges The Finnish Funding Agency for Technology and Innovation (TEKES, project 1297/31/2016) and the Huonekalusäätio (2014, 2015) for financial support. X.W. thanks The Finnish Cultural Foundation for providing the personal grant. L.M.B. acknowledges the Academy of Finland (decision 268616) and the Orion Research Foundation. The authors thank the following people: Ms. Ritva Kivelä for fluidizing CNF; Prof. M. Skurnik for kindly providing *S. aureus* strain MRSA 14TK301; Prof. V. Cerullo and M.Sc. M. Fusciello for access to research facilities, human fibroblasts, and human whole blood (Red Cross, Finland). The authors also acknowledge the Electron Microscopy Unit of the Institute of Biotechnology, University of Helsinki, for facilitating the scanning electron microscopy.

■ REFERENCES

(1) Banerjee, I.; Pangule, R. C.; Kane, R. S. Antifouling coatings: recent developments in the design of surfaces that prevent fouling by proteins, bacteria, and marine organisms. *Adv. Mater.* **2011**, *23*, 690−718.

(2) Tuson, H. H.; Weibel, D. B. Bacteria-surface interactions. *Soft Matter* **2013**, *9*, 4368−4380.

(3) Epstein, A. K.; Wong, T.-S.; Belisle, R. A.; Boggs, E. M.; Aizenberg, J. Liquid-infused structured surfaces with exceptional anti-biofouling performance. *Proc. Natl. Acad. Sci. U. S. A.* **2012**, *109*, 13182−13187.

(4) Mi, L.; Jiang, S. Integrated antimicrobial and nonfouling zwitterionic polymers. *Angew. Chem., Int. Ed.* **2014**, *53*, 1746−1754.

(5) Flynn, P. B.; Gilmore, B. F. Understanding plasma biofilm interactions for controlling infection and virulence. *J. Phys. D: Appl. Phys.* **2018**, *51*, 263001.

(6) Hasan, J.; Crawford, R. J.; Ivanova, E. P. Antibacterial surfaces: the quest for a new generation of biomaterials. *Trends Biotechnol.* **2013**, *31*, 295−204.

(7) Hosseinidoust, Z.; Olsson, A. L. J.; Tufenkji, N. Going viral: Designing bioactive surfaces with bacteriophage. *Colloids Surf., B* **2014**, *124*, 2−16.

(8) Ren, W.; Cheng, W.; Wang, G.; Liu, Y. Developments in antimicrobial polymers. *J. Polym. Sci., Part A: Polym. Chem.* **2017**, *55*, 632−639.

(9) Choi, I.; Lee, J.; Kim, W.; Kang, H.; Bae, S. W.; Chang, R.; Kim, S.; Yeo, W.-S. On-demand modulation of bacterial cell fates on

multifunctional dynamic substrates. *ACS Appl. Mater. Interfaces* **2018**, *10*, 4324−4332.
(10) Klemm, D.; Heublein, B.; Fink, H.-P.; Bohn, A. Cellulose: Fascinating Biopolymer and Sustainable Raw Material. *Angew. Chem., Int. Ed.* **2005**, *44*, 3358−3393.
(11) Kontturi, E.; Laaksonen, P.; Linder, M. B.; Nonappa; Gröschel, A. H.; Rojas, O. J.; Ikkala, O. Advanced materials through assembly of nanocelluloses. *Adv. Mater.* **2018**, *30*, 1703779.
(12) Missoum, K.; Belgacem, M. N.; Bras, J. Nanofibrillated cellulose surface modification: A Review. *Materials* **2013**, *6*, 1745−1766.
(13) Zhang, Y.; Nypelö, T.; Salas, C.; Arboleda, J.; Hoeger, I. C.; Rojas, O. J. Cellulose nanofibrils: From strong materials to bioactive surfaces. *J. Renew. Mater.* **2013**, *1*, 195−211.
(14) Lin, N.; Dufresne, A. Nanocellulose in biomedicine: Current status and future prospect. *Eur. Polym. J.* **2014**, *59*, 302−325.
(15) Chen, W.; Yu, H.; Lee, S.-Y.; Wei, T.; Li, J.; Fan, Z. Nanocellulose: a promising nanomaterial for advanced electrochemical energy storage. *Chem. Soc. Rev.* **2018**, *47*, 2837−2872.
(16) Tavakolian, M.; Okshevsky, M.; van de Ven, T. G. M.; Tufenkji, N. Developing antibacterial nanocrystalline cellulose using natural antibacterial agents. *ACS Appl. Mater. Interfaces* **2018**, *10*, 33827−33838.
(17) Miller, J. *Nanocellulose: Technology, Applications and Markets*; Special Market Analysis Study, RISI, 2014.
(18) Österberg, M.; Vartiainen, J.; Lucenius, J.; Hippi, U.; Seppälä, J.; Serimaa, R.; Laine, J. A Fast method to produce strong NFC films as a platform for barrier and functional materials. *ACS Appl. Mater. Interfaces* **2013**, *5*, 4640−4647.
(19) Ning, R.; Wu, C.-N.; Takeuchi, M.; Saito, T.; Isogai, A. Preparation and characterization of zinc oxide/TEMPO oxidized cellulose nanofibril composite films. *Cellulose* **2017**, *24*, 4861−4870.
(20) Lizundia, E.; Goikuria, U.; Vilas, J. L.; Cristofaro, F.; Bruni, G.; Fortunati, E.; Armentano, I.; Visai, L.; Torre, L. Metal Nanoparticles Embedded in Cellulose Nanocrystal Based Films: Material Properties and Post-use Analysis. *Biomacromolecules* **2018**, *19*, 2618−2628.
(21) Diez, I.; Eronen, P.; Österberg, M.; Linder, M. B.; Ikkala, O.; Ras, R. H. Functionalization of nanofibrillated cellulose with silver nanoclusters: fluorescence and antibacterial activity. *Macromol. Biosci.* **2011**, *11*, 1185−1191.
(22) Missoum, K.; Sadocco, P.; Causio, J.; Belgacem, M. N.; Bras, J. Antibacterial activity and biodegradability assessment of chemically grafted nanofibrillated cellulose. *Mater. Sci. Eng., C* **2014**, *45*, 477−483.
(23) Yu, H.-Y.; Yang, X.-Y.; Lu, F.-F.; Chen, G.-Y.; Yao, J.-M. Fabrication of multifunctional cellulose nanocrystals/poly(lactic acid) nanocomposites with silver nanoparticles by spraying method. *Carbohydr. Polym.* **2016**, *140*, 209−219.
(24) Saini, S.; Sillard, C.; Belgacem, M. N.; Bras, J. Nisin anchored cellulose nanofibers for long term antimicrobial active food packaging. *RSC Adv.* **2016**, *6*, 12422−12430.
(25) Saini, S.; Belgacem, M. N.; Bras, J. Effect of variable aminoalkyl chains on chemical grafting of cellulose nanofiber and their antimicrobial activity. *Mater. Sci. Eng., C* **2017**, *75*, 760−768.
(26) SCENIHR (Scientific Committee on Emerging and Newly Identified Health Risks) *Nanosilver: safety, health and environmental effects and role in antimicrobial resistance*, June 16th, 2014, ISSN: 1831-4783, DOI: 10.2772/76851.
(27) Panacek, A.; Kvitek, L.; Smekalova, M.; Vecerova, R.; Kolar, M.; Roderova, M.; Dycka, F.; Sebela, M.; Prucek, R.; Tomanec, O.; Zboril, R. Bacterial resistance to silver nanoparticles and how to overcome it. *Nat. Nanotechnol.* **2018**, *13*, 65−71.
(28) Fallarero, A.; Skogman, M.; Kujala, J.; Rajaratnam, M.; Moreira, V. M.; Yli-Kauhaluoma, J.; Vuorela, P. (+)-Dehydroabietic acid, an abietane-type diterpene, inhibits *Staphylococcus aureus* biofilms *in vitro*. *Int. J. Mol. Sci.* **2013**, *14*, 12054−12072.
(29) Pirttimaa, M.; Nasereddin, A.; Kopelyanskiy, D.; Kaiser, M.; Yli-Kauhaluoma, J.; Oksman-Caldentey, K.-M.; Brun, R.; Jaffe, C. L.; Moreira, V. M.; Alakurtti, S. Abietane-Type Diterpenoid Amides with Highly Potent and Selective Activity against *Leishmania donovani* and *Trypanosoma cruzi*. *J. Nat. Prod.* **2016**, *79*, 362−368.
(30) Laine, J.; Lindström, T.; Nordmark, G. G.; Risinger, G. Studies on topochemical modification of cellulosic fibres. Part 1. Chemical conditions for the attachment of carboxymethyl cellulose onto fibres. *Nord. Pulp Pap. Res. J.* **2000**, *15*, 520−526.
(31) Prat, D.; Wells, A.; Hayler, J.; Sneddon, H.; McElroy, C. R.; Abou-Shehada, S.; Dunn, P. J. CHEM21 selection guide of classical- and less classical-solvents. *Green Chem.* **2016**, *18*, 288−296.
(32) Rossky, P. J.; Earis, P.; Hordern, J.; Nugent, N.; Patel, V.; Lunn, H.; Roffey, A. *Faraday Discuss.* **2010**, *146*, 13−18.
(33) Lozhechnikova, A.; Bellanger, H.; Michen, B.; Burgert, I.; Österberg, M. Surfactant-free carnauba wax dispersion and its use for layer-by-layer assembled protective surface coatings on wood. *Appl. Surf. Sci.* **2017**, *396*, 1273−1281.
(34) Kim, D.; Seo, J. A review: Breathable films for packaging applications. *Trends Food Sci. Technol.* **2018**, *76*, 15−27.
(35) *Moisture Buffering of Building Materials*, Report BYG·DTU R-126; Rode, C., Ed.; Technical University of Denmark (DTU), 2005.
(36) Peresin, M. S.; Kammiovirta, K.; Heikkinen, H.; Johansson, L.-S.; Vartiainen, J.; Setälä, H.; Österberg, M.; Tammelin, T. Understanding the mechanisms of oxygen diffusion through surface functionalized nanocellulose films. *Carbohydr. Polym.* **2017**, *174*, 309−317.
(37) Alexander, M. R.; Williams, P. Water contact angle is not a good predictor of biological responses to materials. *Biointerphases* **2017**, *12*, 02C201.
(38) Freudenberg, U.; Zimmermann, R.; Schmidt, K.; Behrens, S. H.; Werner, C. Charging and swelling of cellulose films. *J. Colloid Interface Sci.* **2007**, *309*, 360−365.
(39) Olszewska, A.; Junka, K.; Nordgren, N.; Laine, J.; Rutland, M. W.; Österberg, M. Non-ionic assembly of nanofibrillated cellulose and polyethylene glycol grafted carboxymethyl cellulose and the effect of aqueous lubrication in nanocomposite formation. *Soft Matter* **2013**, *9*, 7448−7457.
(40) Zimmermann, R.; Dukhin, S. S.; Werner, C.; Duval, J. F.L. On the use of electrokinetics for unravelling charging and structure of soft planar polymer films. *Curr. Opin. Colloid Interface Sci.* **2013**, *18*, 83−92.
(41) Swerin, A.; Odberg, L.; Lindström, T. Deswelling of hardwood kraft pulp fibers by cationic polymers. The effect on wet pressing and sheet properties. *Nord. Pulp Pap. Res. J.* **1990**, *5*, 188−196.

DOI: 10.1021/acssuschemeng.8b05658
ACS Sustainable Chem. Eng. 2019, 7, 5002−5009